Research Article

Yasir M. Al-Badran*, Wiebke Baille and Tom Schanz†

One dimensional normal consolidation line equation

https://doi.org/10.1515/jmbm-2022-0234
received April 14, 2022; accepted May 23, 2022

Abstract: Many empirical equations have been proposed in the past to predict the parameters of the one-dimensional normal consolidation line (1D-NCL) for soils. However, applications of these equations are limited to specific range of pressure and plasticity soils. General empirical equations for 1D-NCL for large range of pressure and plasticity soils are presented in this study. It is assumed that the 1D-NCL has up to three slopes and these slopes start at different stresses depending on liquid limit (LL) of soils. The 1D-NCL of 59 different soils for a large range of LL (19–520%) was used to establish the initial part of 1D-NCL. The soils were categorized based on their LL into two groups: (i) LL < 110% and (ii) LL > 110%. The equations for initial part of 1D-NCL were compared with the previous empirical 1D-NCL equations. The comparisons showed that the new 1D-NCL equations have a better agreement with tests results, especially for highly plastic soils. Moreover, two soils with different plasticity were used to verify the new 1D-NCL equations. The verifications showed a good agreement between the experimental and the predicted results.

Keywords: normal consolidation line, consolidation, volume change, liquid limit

1 Introduction

The complete one-dimensional normal consolidation line (1D-NCL) for soils (for low and high range of pressure and plasticity soils) is important to simulate yielding volume change surface, compaction curve, settlement, high swelling pressure of the buffer/backfilling material for nuclear and toxic wastes, and the soil-water characteristic curve (SWCC) [1,2]. This point will be discussed further in Section 3. Several empirical equations have been proposed in literature to predict the parameters of the equation for the 1D-NCL for soils in logarithmic scale (e–log σ_v' plot), but the proposed relations deal with low and medium ranges of (i) plastic soils (LL: 20–200%) and (ii) stresses (till 800 kPa). Regarding the experimental results in literature [1–6] and the theoretical work based on the diffuse double layer theory [7,8], it is well known that the 1D-NCL changes its slope (C_c) at high effective stresses especially for highly plastic soils. The experimental results showed that NCL has different behavior with regards to the physical-chemical (or plasticity) properties of soil, Figure 1. Figure 1 shows the complete 1D-NCL for 11 soils from literature used in this study [2,3,6,8–10]. These tests were carried out with stress ranging from minimum up to 24 MPa. Thus, the 1D-NCL equation of one (or constant) slope (C_c) does not represent the compression behavior of soil at high effective stresses especially in high plastic soils. In this study, it is assumed that the 1D-NCL has up to three slopes and these slopes start at different stresses, Figure 2, depending on liquid limit (LL) of soils. This assumption with the new proposed set of equations presents a novel approach for predicting the 1D-NCL. Figure 2 presents the proposed complete 1D-NCL with three slopes C_{c1}, C_{c2}, and C_{c3}. Even though the motivations of the study depend on the previous experimental results and theoretical work, the outcome equations are empirical based on statistic (regression) analysis.

This study aims to establish the general empirical equations for 1D-NCL for large range of stresses and plastic soils.

2 Literature review

Nagaraj and Murthy Srinivasa [11] stated that the 1D-NCL equation can be written as

† Deceased.

*** Corresponding author: Yasir M. Al-Badran,** Department of Civil Engineering, Mustansiriyah University, Baghdad, Iraq, e-mail: yasiralbadran@uomustansiriyah.edu.iq
Wiebke Baille: Department of Soil Mechanics Foundation Engineering and Environmental Geotechniques, Ruhr-Universität Bochum, Bochum, Germany, e-mail: Wiebke.Baille@rub.de
Tom Schanz: Ruhr-Universität Bochum, Bochum, Germany

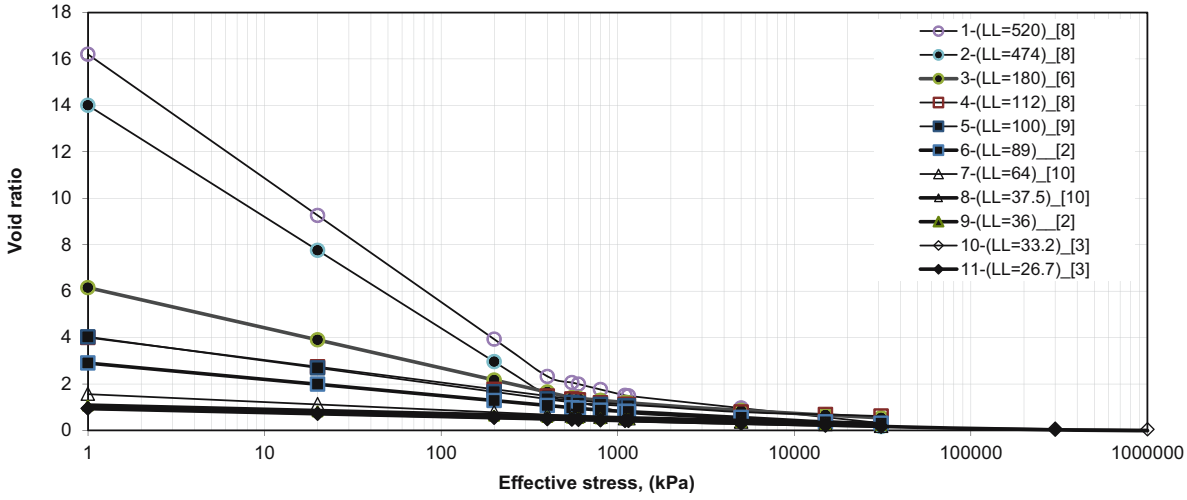

Figure 1: The complete 1D-NCL for 11 soils used in this study.

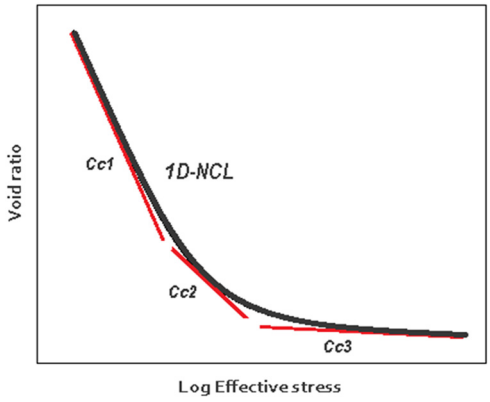

Figure 2: The proposed complete 1D-NCL with three slopes C_{c1}, C_{c2}, and C_{c3}.

$$e_{NCL} = N - C_c \log \sigma', \quad (1)$$

where e_{NCL} = void ratio of 1D-NCL; N = void ratio of 1D-NCL at 1 kPa; C_c = compression index (slope) of 1D-NCL when σ' in logarithmic scale; and σ' = effective stress.

Plasticity and compressibility are characteristic properties of clays. Atterberg limits of a fine-grained (clayey) soil reveal the nature and amount of clay minerals present [12].

Many different empirical correlations between the parameters of the 1D-NCL equation (N and C_c) and index properties of soils (LL and plastic limit [PL]) have been proposed in literature. Skempton [13] suggested a relationship between compression index (C_c) and LL (C1 in Table 1) by conducting consolidation tests on remolded soil specimens of several diverse types of clay with water content starting from LL. The equation of compression index, C_c, is adapted form for the clay soils in the normally consolidated state proposed in [14], (C2 in Table 1). Other relationships between compression index and initial void ratio (e_o) have been proposed by [15] on the basis of stress–strain considerations and the slope of the consolidation curves (*C*3 and *C*4 in Table 1). Hough [16] proposed double diverse empirical equations to evaluate compression index for organic soils (not mentioned in the table) and mineral soils (*C*5 in Table 1). Azzouz *et al.* [17] derived empirical equations concerning compression index and water content, *in situ* void ratio, and LL (*C*6a and *C*6b in Table 1). Bowles [18] reported many empirical equations some of them related to the Brazilian soils, and others related to the organic soils, and for soils with low plasticity (*C*7 in Table 1). A unique compression index equation was suggested in [19] based on the statistical analysis of extensive data (*C*8 in Table 1). Mayne [20] presented equation for compression index depending on LL for clays (*C*9 in Table 1). A relation among the natural water content and compression index was reported in [21] for Chicago clays and Alberta clays (*C*10 Table 1). Nagaraj and Murthy Srinivasa [11] established an empirical relationship between the ratio e/e_L and σ_v' (e_L = G·LL) based on considerations of physical chemistry for different natural soils for LL approximately from 36 to 160% (*N*1 and *C*12 in Table 1). Burland [22] made attempt to predict the compression characteristics of natural soils depending on void ratio of LL e_L by making use of empirical correlations between the Atterberg limits and the intrinsic constants of compressibility e_{100} (void ratio at 100 kPa) and C_c (*N*2 and *C*12 in Table 1). Nath and DeDalal [23] carried out many consolidation tests on mixed soil samples (LL 19–205%), starting from approximately LL water content, to produce correlation among the compression characteristics and plasticity index of several soils (*N*3 and *C*13 in Table 1). Al-Khafaji [24] reported a statistical

Table 1: Parameters of 1D-NCL equation (N and C_c) for the previous works

References	N		C_c		Soil type
Skempton [13]		—	*Cc*-1	0.007 (LL% − 10)	Remolded clays
Terzaghi and Peck [14]		—	*Cc*-2	0.009 (LL% − 10)	NC soils moderately sensitive
Nishida [15]		—	*Cc*-3	1.15 (e − 0.35)	Clays
Nishida [15]		—	*Cc*-4	0.45 (e_o − 0.35)	Natural soils
Hough [16]		—	*Cc*-5	0.30 (e_o − 0.27)	Inorganic silty sand-silty clay
Azzouz *et al.* [17]		—	*Cc*-6a + *Cc*-6b	0.37 (e_o + 0.003LL − 0.34) 0.4 (e_o + 0.001w_n − 0.25)	
Bowles [18]		—	*Cc*-7	0.75 (e_o − 0.50)	Soils with low plasticity
Oswald [19]		—	*Cc*-8	0.5 $(\gamma_w/\gamma_d{}^2)^{1.2}$	Clays
Mayne [20]		—	*Cc*-9	(LL − 13)/109	Clays
Koppula [21]		—	*Cc*-10	0.01(w_n%)	Chicago and Alberta clays
Nagaraj and Murthy Srinivasa [11]	*N*1	1.122(e_L)	*Cc*-11	0.2343(e_L)	Different types for soils of LL (36.2–160%)
Burland [22]	*N*2	e_{100} = 0.109 + 0.679e_L − 0.089e_{L2} + 0.016e_{L3}	*Cc*-12	0.256e_L − 0.04	Soils of LL (25–160%) and above A-line
Nath and DeDalal [23]	*N*3	((C_c + 0.2117)/0.5269) − C_c * log (1/20)	*Cc*-13	0.0124 (LL − 0.1761)	Soils of LL (19–205%)
Al-Khafaji [24]		—	*Cc*-14	0.009 (LL − 16)	Soils of LL (16–200%)

Note: N = void ratio of NCL at 1 kPa; C_c = compression index of NCL; LL% = liquid limit in percentage; e_o = initial or *in situ* void ratio; w_n = natural water content; γ_w = unit weight of water; γ_d = dry unit weight of soil at which C_c is required; e_L = G * LL; G = specific gravity, e_{100} = void ratio at 100 kPa effective stress.

relationship between compression index and LL (*C*14 in Table 1). There are similar other relationships given by several researchers, but for specific soils (*i.e.*, organic soils in [18]) or specific regions (*i.e.*, [18,25,26]) will not report here.

Al-Khafaji [24] stated that: (i) Evaluation of published data and compression index equations conclude that every equation among compression index and soil index properties is only approximate; (ii) Nevertheless, these approximate values are significant in preliminary studies of settlement and offer a specific indication in order to evaluate the compression index value; (iii) The common empirical equations in literature have a linear relation among compression index, LL, natural water content, and *in situ* void ratio; (iv) No attention were made to the effect of errors that can be related to the human operator skill, the determinations of void ratio and water content, sample size, load increments, time increments, *etc*., and these could be significant.

3 Needs of NCL at high stresses range

The conventional 1D-consolidation tests are carried out to determine the compressibility behavior of soils up to a vertical stress of about 800 kPa. Numerous countries plan to bury the toxic waste facilities at large depths ranging from 500 to 1,000 m below ground level bordered by host rock completely [27,28]. According to the study of Tripathy *et al.* [7], the usual overburden soil density is 1.8 Mg/m^3, and the geostatic pressure in these depths is estimated to be about 9.0–16.0 MPa. At these depths, high compacted soils (almost bentonites) are used to function as a barrier for the toxic wastes. Furthermore, compacted bentonites are also recommended for use as buffer/backfilling materials for sealing the tunnels and the access galleries. When the fluid from the saturated host rock contact with the buffrer, the high compacted bentonites swell and the stress–void ratio relation of the compacted saturated bentonites, as well as the stress conjunction of the host rock, become key issues in this scenario. Moreover, the complete 1D-NCL (at low and high stress ranges) is important to simulate yielding volume change surface, compaction curve, settlement and the SWCC [1,2].

As a result, various researchers have lately reported extensive research investigations on the hydro-mechanical behavior of swelling clays with a broad range of dry densities due to substantial pressure and suction variations [1,2,5,6,29–31]. Given the wide range of dry densities of relevance to practicing geotechnical engineers, it is required to apply very high stress in the laboratory to

Table 2: The NCL properties of 59 different soils used in this study

No.	Soils	G	LL%	e_L	N	C_{c1}	C_{c2}	C_{c3}	Start C_{c2} [kPa]	Start C_{c3} [kPa]	References
1	Na-Ca MX80	2.65	520	13.78	16.2	5.335	1.85	0.82	400	1,100	[5]
2	Na-Kunigel	2.79	472	13.169	14	4.8	1.7	0.4	400	1,150	[5]
3	100B-0S	2.75	206	5.654	8	2.3	—	—	—	—	[23]
4	100B2	2.8	180	5.04	6.15	1.73	0.7	0.4	550	2,000	[6]
5	90B-10S	2.74	179	4.9046	6.939	2	—	—	—	—	[23]
6	80B-20S	2.73	161	4.3953	6.225	1.8	—	—	—	—	[23]
7	Sail soil	2.8	159	4.4604	5.25	1.2	—	—	—	—	[11]
8	70B-30B	2.72	142	3.8624	5.471	1.62	—	—	—	—	[23]
9	Whangamarine clay	2.80	136	3.808	4.45	0.87	—	—	—	—	[11]
10	Little bell clay	2.70	126	3.402	4.2	0.86	—	—	—	—	[11]
11	60B-40S	2.71	121	3.2791	4.638	1.3	—	—	—	—	[23]
12	Ca Fourges	2.67	112	2.9904	4	0.968	0.8	0.22	600	5,000	[5]
13	100composite clay-0S	2.73	101	2.7624	3.845	1	—	—	—	—	[23]
14	50B-50S	2.70	100	2.7	3.805	1.05	—	—	—	—	[23]
15	Soil 4	2.60	100	2.6	4.03	1.03	0.41	—	600	—	[9]
16	Black cotton	2.81	97	2.734	3.2	0.7	—	—	—	—	[11]
17	100B1	2.75	89	2.4475	2.9	0.7018	0.4	0.177	700	15,000	[1]
18	85composite clay-15S	2.72	83	2.2595	3.131	0.82	—	—	—	—	[23]
19	40B-60S	2.69	80	2.152	3.012	0.8	—	—	—	—	[23]
20	Soft clay	2.8	78	2.184	2.5	0.52	—	—	—	—	[11]
21	Silty clay	2.75	69	1.8975	2.101	0.43	—	—	—	—	[11]
22	70composite clay-30S	2.71	69	1.856	2.556	0.725	—	—	—	—	[23]
23	Soil 3	2.60	65	1.65	2.35	0.5	—	—	—	—	[9]
24	50B2	2.72	64	1.744	1.56	0.34	0.22	0.14	1,500	17,000	[1]
25	Thomasville	2.75	60	1.65	1.756	0.339	—	—	—	—	[19]
26	Silty clay	2.65	59	1.5741	1.563	0.29	—	—	—	—	[11]
27	Residual clay	2.80	59	1.652	1.684	0.31	—	—	—	—	[11]
28	30B-70S	2.68	59	1.5812	2.179	0.5	—	—	—	—	[23]
29	St Clair river	2.74	57	1.56	1.603	0.29	—	—	—	—	[19]
30	55composite clay-45S	2.70	55	1.4832	2.020	0.58	—	—	—	—	[23]
31	Nr 3	2.6	47	1.22	1.335	0.27	—	—	—	—	[19]
32	100Kaolin-0S	2.68	47	1.2542	1.695	0.305	—	—	—	—	[23]
33	Vienna clay	2.70	47	1.2609	1.48	0.32	—	—	—	—	[11]
34	Galisteo dam	2.72	46	1.25	1.331	0.26	—	—	—	—	[19]
35	Red soil	2.70	45	1.2231	1.341	0.28	—	—	—	—	[11]
36	Soil 2	2.59	45	1.1681	1.31	0.16	—	—	—	—	[9]
37	20B-80S	2.67	45	1.1882	1.604	0.30	—	—	—	—	[23]
38	90kaolin-10S	2.67	43	1.1431	1.523	0.26	—	—	—	—	[23]
39	Artificial silt	2.7	42	1.1205	1.216	0.20	—	—	—	—	[33]
40	40composite clay-60S	2.68	40	1.0602	1.405	0.415	—	—	—	—	[23]
41	30B2	2.75	38	1.0106	1.09	0.18	0.16	—	15,000	—	[1]
42	80kaolin-20S	2.67	37	0.9760	1.286	0.21	—	—	—	—	[23]
43	Silty sand	2.70	36	0.9774	1.05	0.20	—	—	—	—	[11]
44	30B1	2.70	30	0.9702	1.059	0.19	0.165	—	15,000	—	[1]
45	Lower Clinton river	2.77	35	0.97	0.813	0.098	—	—	—	—	[19]
46	Till1	2.76	33.2	0.9163	0.937	0.179	0.12	0.06	20,000	75,000	[3]
47	Sandy clay	2.73	33	0.9009	0.85	0.17	—	—	—	—	[34]
48	25composite clay-75S	2.61	33	0.8815	1.148	0.19	—	—	—	—	[23]
49	70kaolin-30B	2.67	32	0.8547	1.108	0.20	—	—	—	—	[23]
50	Residual soil	2.69	31	0.8339	0.89	0.135	—	—	—	—	[35]
51	Soil 1	2.6	29	0.7618	1	0.2	—	—	—	—	[9]
52	20composite clay-80S	2.67	30	0.7868	1.009	0.10	—	—	—	—	[23]
53	Bloomington dam	2.69	29	0.7801	0.788	0.136	—	—	—	—	[19]
54	60kaolin-40S	2.67	28	0.7471	0.949	0.16	—	—	—	—	[23]
55	Silt	2.72	27	0.7262	0.936	0.17	0.152	0.058	60,000	300,000	[3]
56	10B-90S	2.66	26	0.6916	0.870	0.10	—	—	—	—	[23]

(*Continued*)

Table 2: *Continued*

No.	Soils	G	LL%	e_L	N	C_{c1}	C_{c2}	C_{c3}	Start C_{c2} [kPa]	Start C_{c3} [kPa]	References
57	50kaolin-50S	2.67	25	0.6663	0.830	0.145	—	—	—	—	[23]
58	40kaolin-60S	2.66	22	0.5856	0.711	0.13	—	—	—	—	[23]
59	30kaolin-70S	2.66	19	0.5052	0.592	0.095	—	—	—	—	[23]

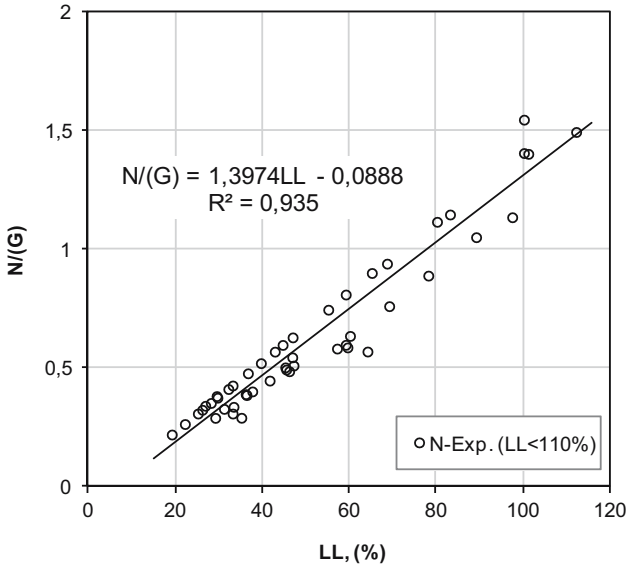

Figure 3: Best-fit relationship of *N/G versus* LL < 110%.

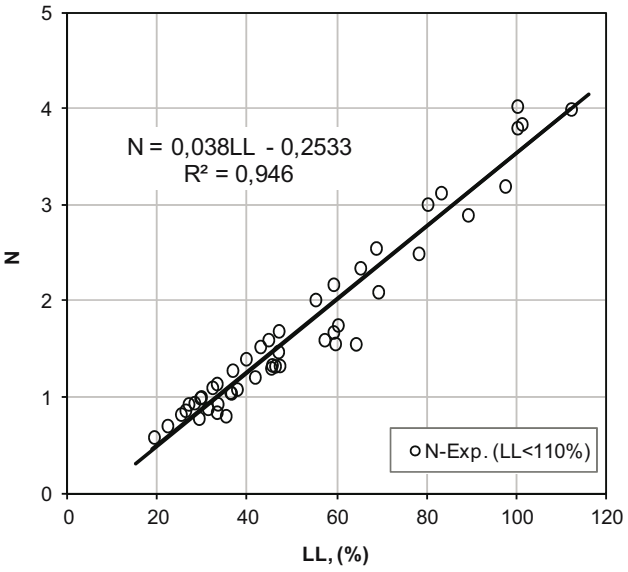

Figure 5: Best-fit relationship of *N vs* LL < 110%.

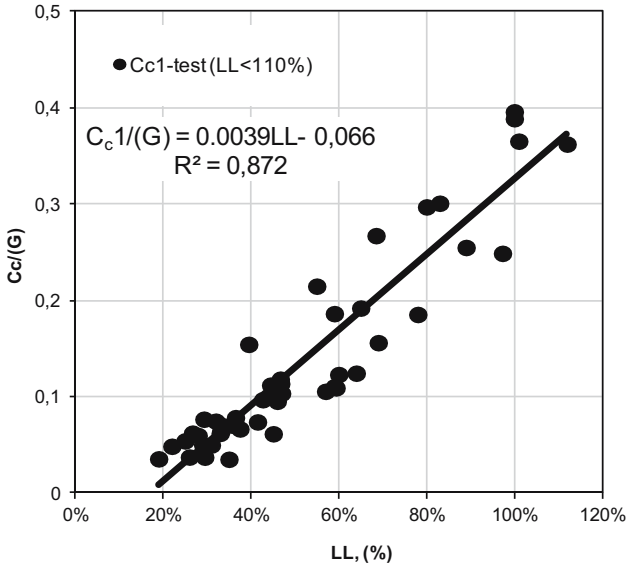

Figure 4: Best-fit relationship of C_{c1}/G *versus* LL < 110%.

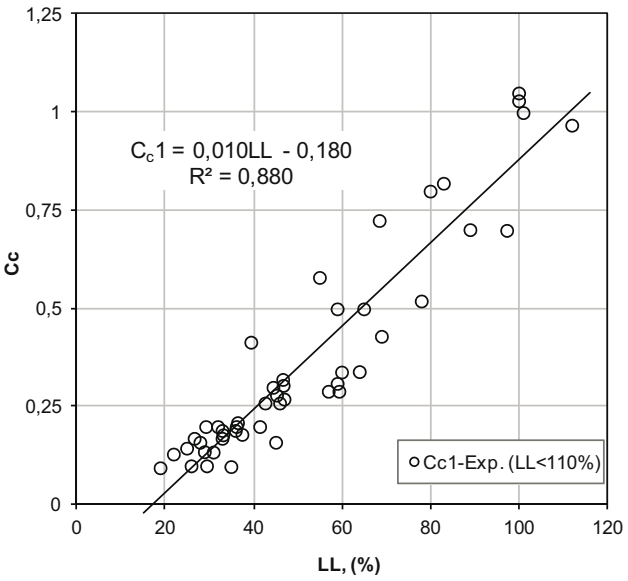

Figure 6: Best-fit relationship of C_{c1} *vs* LL < 110%.

assess the volume change characteristic of the clays. It should be noted that determining the compressibility behavior at extremely high stresses necessitates the use of special heavy equipment and loading mechanisms, in addition to the fact that the test duration is substantially longer due to the increased number of loading stages [7].

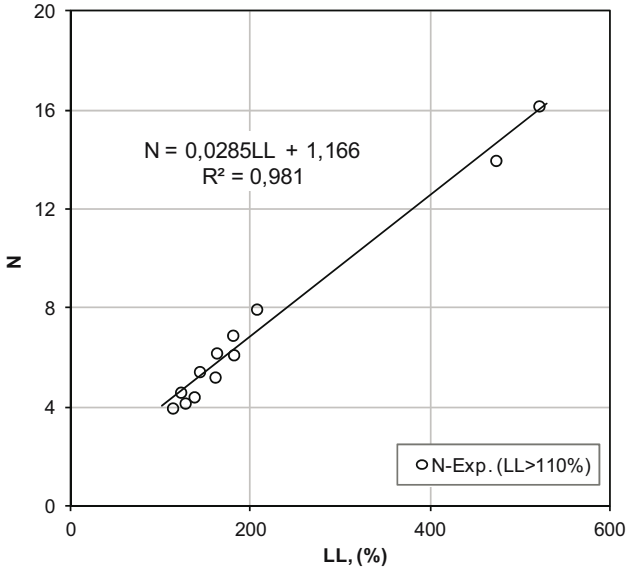

Figure 7: Best-fit relationship of *N vs* LL > 110% (12 different soils).

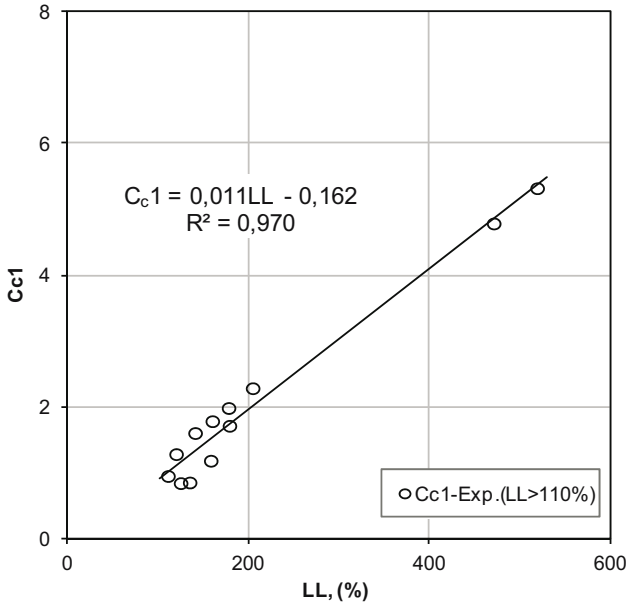

Figure 8: Best-fit relationship of C_{c1} *vs* LL > 110% (12 different soils).

4 New empirical equations for the complete NCL

Nagaraj and Murthy Srinivasa [11] stated that the relation of normalized void ratio (the ratio of the void ratio [e] to the void ratio of LL [e_L]) *vs* the net repulsive pressure (R-A) relationship is further common and fundamental than half-space distance (d) *vs* (R-A) relation. Therefore, in this study, the void ratio of LL (e_L) or multiplying specific gravity with LL (G * LL) is used first as soil parameter to establish the 1D-NCL equation. So, in other form, the relations (G *vs* N/LL) and (G *vs* C_c/LL) are investigated. Note that the value of N (the void ratio at 1 kPa) is obtained by extending the straight line of NCL till 1 kPa.

Investigating the relationship of terms N/G and C_c/G *vs* large range of LL for 59 different soils (Table 2) with LL in the range of 19–520% shows that the best-fit equations can be obtained by dividing the LL range into two groups. Table 2 presents the NCL properties of 59 different soils used in this study. The value of 110% LL shows as a best limit between the two groups for both the relations (*i.e.*, N and C_c). Therefore, the soils are categorized into two

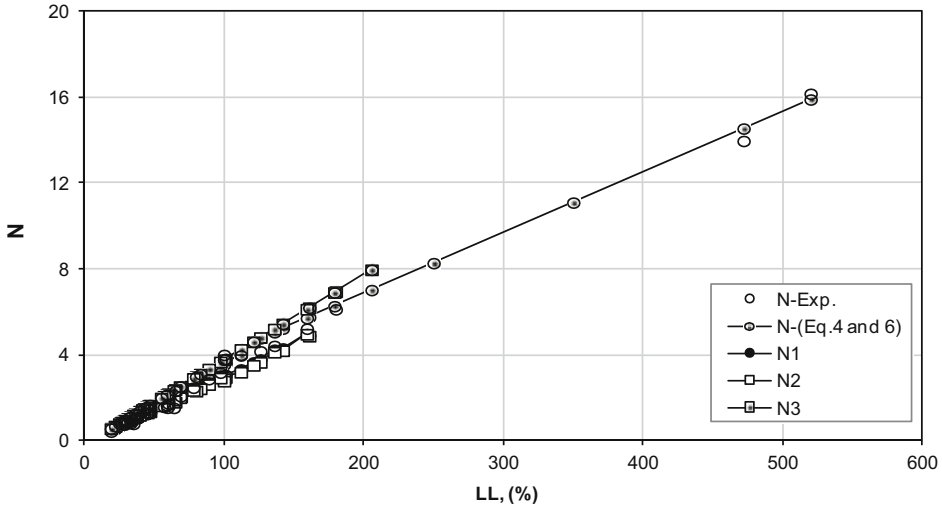

Figure 9: The comparison between the new Eqs. (4)–(6) of *N vs* complete range of LL and the other previous empirical equations in Table 1 for the given 59 different soils used in this study.

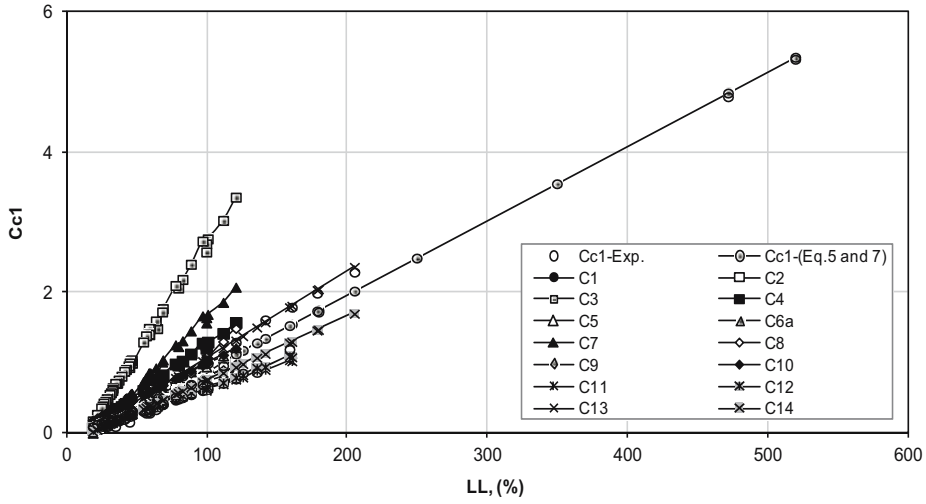

Figure 10: The comparison between the new Eqs. (5)–(7) of C_{c1} *vs* complete range of LL and the other previous empirical equations in Table 1 for the given 59 different soils used in this study.

groups: (*i*) soils with LL < 110% and (*ii*) soils with LL > 110%. This categorization is adopted due to the experimental results which show that the 1D-NCL of soils with LL < 110% (group *i*) has only one slope, while the 1D-NCL of soils with LL > 110% (group *ii*) has more than one slope, the experimental results are shown in Figures 3 and 4. Such behavior can be attributed to the physico-chemical properties of soils, *i.e.*, existing of a significant amount of montmorillonite and illite minerals in soils when LL > 110%. Lambe and Whitman [32] cited that the LL values mainly for montmorillonite and illite minerals are more than 110%. Moreover, the experimental results show that the 1D-NCL of high plasticity soils changes its slope at stresses varying based on the soil plasticity (*i.e.*, the LL).

The relationships of terms N/G and C_{c1}/G *vs* LL < 110% are shown in Figures 3 and 4. The regression analysis shows that the best-fit equation for term N/G is a linear with $R^2 = 0.9355$ and for term C_{c1}/G is a linear with $R^2 = 0.872$:

$$N_{\mathrm{LL<110\%}} = G(0.014(\mathrm{LL}) - 0.0888), \tag{2}$$

$$C_{\mathrm{c1\,LL<110\%}} = G(0.0039(\mathrm{LL}) - 0.066). \tag{3}$$

The relationship of N and C_c *vs* LL were also investigated. The results show that N and C_c *vs* LL have the same

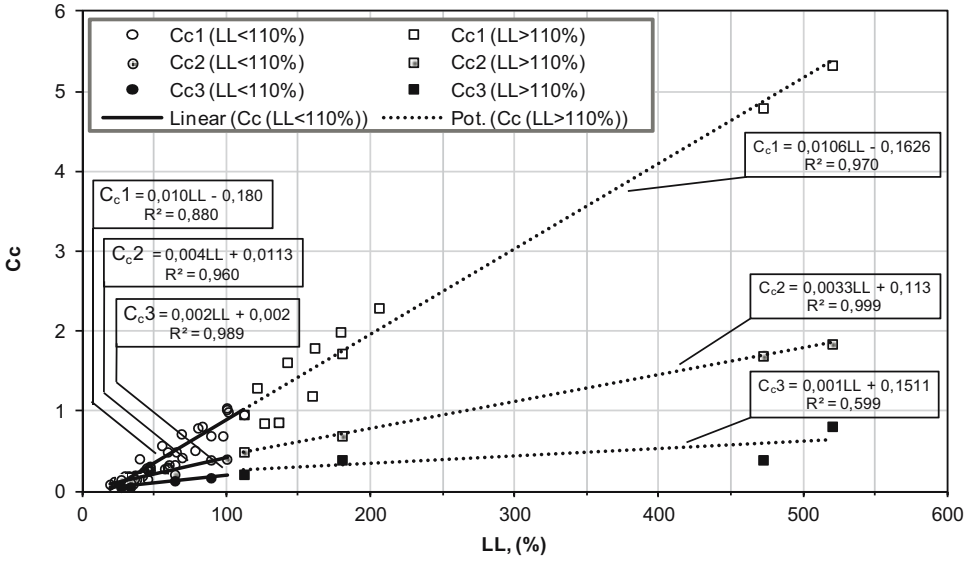

Figure 11: Best-fit relationship of C_c's (C_{c1}, C_{c2}, and C_{c3}) *vs* complete range of LL.

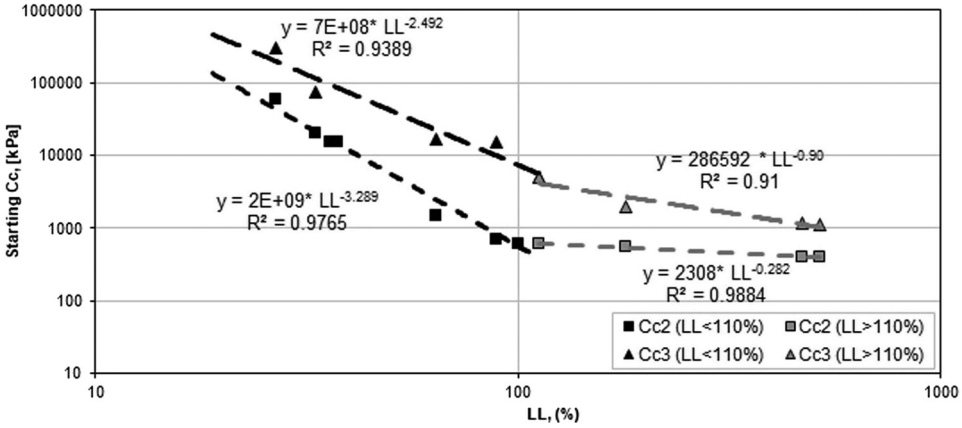

Figure 12: Best-fit relationship of stress for starting C_{c2} and C_{c3} *vs* complete range of LL.

behavior as N/G and C_{c1}/G. Figures 5 and 6 present the relationship of N and C_c *vs* LL < 110%. The regression analysis shows that the best-fit equation for N is a linear with $R^2 = 0.9467$ and for C_c is a linear with $R^2 = 0.88$:

$$N_{LL<110\%} = 3.7962(LL\%/100) - 0.2533, \quad (4)$$

$$C_{c1\,LL<110\%} = 0.0106(LL\%/100) - 0.1806. \quad (5)$$

It is clear from Eqs. (2)–(5) that the LL has the major effect for N and C_{c1} values and they can be predicted depending on the LL value only. Therefore, the N and C_{c1} for the group of LL > 110% will be investigated depending on LL only. However, the second and third slopes of 1D-NCL (C_{c2} and C_{c3}) will also be investigated depending on LL only.

Linear relations are found for N and C_c *vs* LL of 12 different soils (for LL ≥ 110%) as shown in Eqs. (6) and (7) with $R^2 = 0.9817$ and $R^2 = 0.97$, respectively (Figures 7 and 8).

$$N_{LL>110\%} = 2.845(LL\%/100) + 1.1663, \quad (6)$$

$$C_{c1\,LL>110\%} = 1.0635(LL\%/100) - 0.1626. \quad (7)$$

Figures 9 and 10 show the comparison between the new Eqs. (4)–(6) for N and Eqs. (7) and (8) for C_{c1}) and the other previous empirical equations in Table 1 for the given 59 different soils used in this study. As mentioned ahead, the 1D-NCL changes its slope (C_c) at high stresses especially for high plasticity soils. Therefore, any previous empirical equation for 1D-NCL and also the new Eqs. (4)–(8) cannot represent the 1D-NCL for large stresses and high LL range.

This study considers that for each 1D-NCL there are three slopes (*i.e.*, C_{c1}, C_{c2}, and C_{c3}), Figure 2. The slope of tangential line of the initial straight part of 1D-NCL, under low stress range, is considered as C_{c1}. While the slope of tangential line of the final straight part of 1D-NCL, under high stress range, is considered as C_{c3}. The slope of

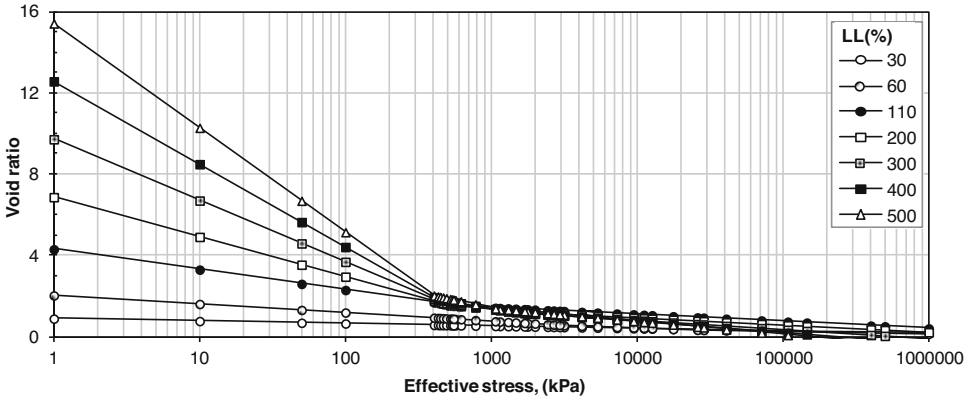

Figure 13: 2D predicted 1D-NCL's for large stresses *vs* LL.

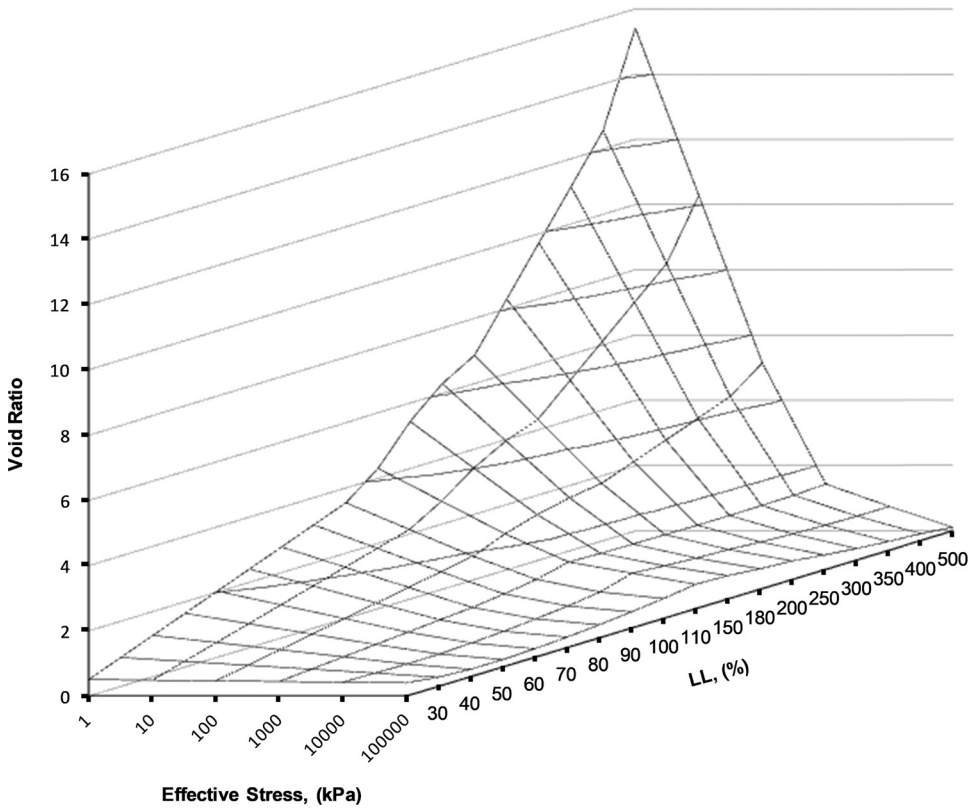

Figure 14: 3D predicted 1D-NCL's for large stresses *vs* LL.

Table 3: Basic properties for Mon-Ca and Mon-Na used in verification (Mesri and Olson [36])

Soil name	pH	LL [%]	PL [%]	Gs	S [m^2/g]
Mon-Ca	7	214	34	2.8	680
Mon-Na	7	1,140	—	2.65	500

tangential line of the intermediate straight part of 1D-NCL, between the range of C_{c1} and C_{c3}, is considered as C_{c2}.

The value of each slope and the stress at the starting of each slope are investigated as shown in Figures 11 and 12. Figure 11 shows that there is a good relationship between C_{c2}, C_{c3}, and LL with the same range of the two groups (before and after 110% LL) as linear function with $R^2 = 0.96$ and 0.999 for C_{c2} (before and after 110% LL) and $R^2 = 0.989$ and 0.599 for C_{c3} (before and after 110% LL).

$$C_{c2(LL<110\%)} = 0.004(LL/100) + 0.0113, \quad (8)$$

$$C_{c2(LL>110\%)} = 0.0033(LL/100) + 0.113, \quad (9)$$

$$C_{c3(LL<110\%)} = 0.002(LL/100) + 0.0002, \quad (10)$$

$$C_{c3(LL>110\%)} = 0.001(LL/100) + 0.1511. \quad (11)$$

Figure 12 shows that the stress at the starting of C_{c2} and C_{c3} must be divided by regrinding LL values into two ranges for a good fitting. Again, the regression analysis shows that the LL value about 110% is the limit to give the best-fit for the stress at the starting of C_{c2} and C_{c3}, respectively, as shown in Eqs. (12)–(15).

$$\sigma'_{C_{c2}(LL<100\%)} = 2 \times 10^9 * (LL)^{-3.28}, \quad (12)$$

$$\sigma'_{C_{c2}(LL>110\%)} = 2{,}308 * (LL)^{-0.282}, \quad (13)$$

$$\sigma'_{C_{c3}(LL<110\%)} = 7 \times 10^8 * (LL)^{-2.492}, \quad (14)$$

$$\sigma'_{C_{c3}(LL>110\%)} = 286{,}592 * (LL)^{-0.9}. \quad (15)$$

Table 4: Calculated parameters of NCL equation for Mon-Ca and Mon-Na using the proposed equations in this study with LL > 110%

Soil name	N (Eq. (6))	C_{c1} (Eq. (6))	C_{c2} (Eq. (9))	σ_C_{c2}(Eq. (13)) [kPa]	σ_C_{c3}(Eq. (15)) [kPa]
Mon-Ca	7.088	2.11	0.120	508	2,290
Mon-Na	33.43	11.96	0.151	317	508

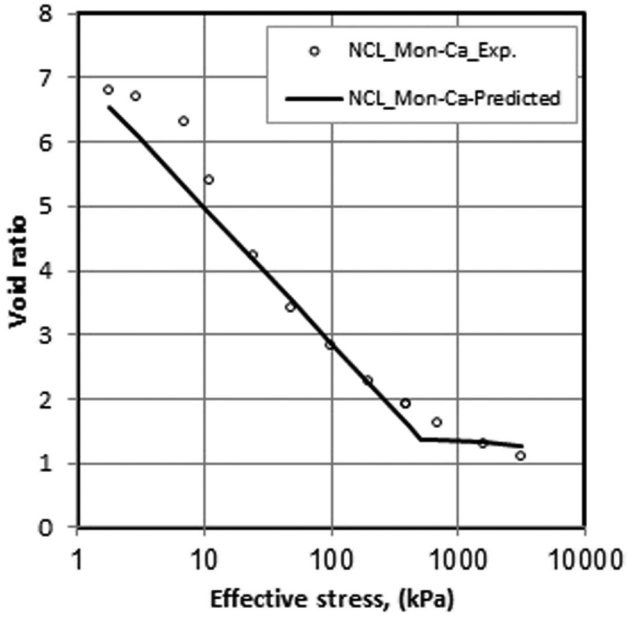

Figure 15: The experimental data and the predicted results of the one-dimensional consolidation tests for the Mon-Ca soil (experimental data from [36]).

The R^2 for the stress at the starting of C_{c2} is 0.976 and 0.988 before and after LL = 110%, whereas the stress at the starting of C_{c3} is 0.938 and 0.913 before and after LL = 110%.

Figures 13 and 14 present the 2D and 3D predicted 1D-NCL's for large stresses *vs* LL, respectively.

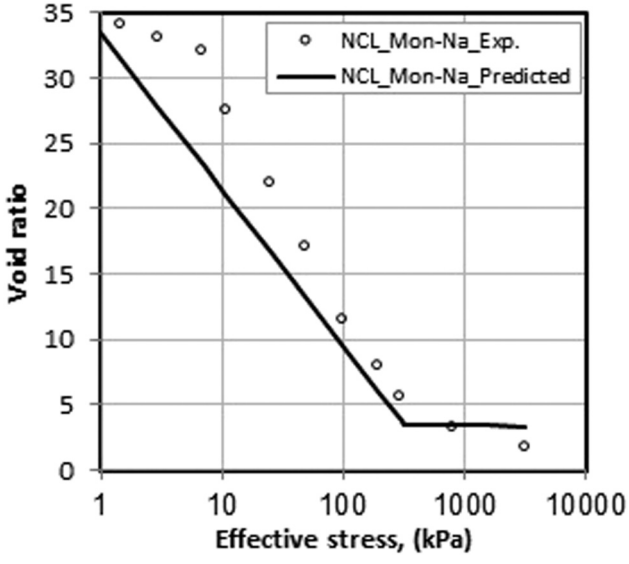

Figure 16: The experimental data and the predicted results of the one-dimensional consolidation tests for the Mon-Na soil (experimental data from [36]).

5 Verification

Two montmorillonite soils (calcium and sodium types) reported in [36] will be used for the verification in this study. The calcium montmorillonite is named Mon-Ca, while the sodium montmorillonite is named Mon-Na. The basic properties of both the soils are presented in Table 3. The LL values are 214 and 1,140% for Mon-Ca and Mon-Na soils, respectively. Thus, both the soils will use the equations for soils with LL > 110 %. The Eqs. (6), (7), (9), (13), and (15) were used to calculate N, C_{c1}, C_{c2}, the stress at the starting of the second slope, and the stress at the starting of the third slope, respectively, as shown in Table 4. Figures 15 and 16 show the experimental data and the predicted results of the one-dimensional consolidation tests for the Mon-Ca and Mon-Na soils. The results show that the predicted NCL's using the proposed equations in this study fit connotatively and qualitatively well with the experimental data. The difference in the initial part between the experimental data and the predicted results in both soils is due to the fact that the predicted results represent the normal consolidated state while the experimental data may represent a slight over consolidated condition. Moreover, two statistic measurements, coefficient of determination (R^2) and mean absolute error (MAE), are used to evaluate the statistic accuracy of the predicted values for the new proposed equations with respect to the experimental data. Due to the over consolidated condition in the low stresses range, the experimental data lower than 25 kPa for the Mon-Ca and the experimental data lower than 50 kPa for the Mon-Na were ignored. The static analysis shows that the R^2 value for Mon-Ca is 0.88 and for Mon-Na is 0.80. While the MAE value for Mon-Ca is 0.335 and for Mon-Na is 2.10.

6 Conclusion

In this study, general empirical equations for 1D-NCL for large range of pressure and plasticity soils are presented. The motivations of the study depend on the previous experimental results and theoretical work, but the outcome equations are empirical based on statistic (regression) analysis for 59 different soils for large range of LL (19–520%). The complete 1D-NCL line assumed has three slopes (C_{c1}, C_{c2}, and C_{c3}). Complete 11 experimental data of 1D-NCL's were used to determine the 2nd and 3rd slopes of NCL (C_{c2} and C_{c3}) and the stress at starting each slope. The equation for initial part of 1D-NCL was

compared with empirical 1D-NCL equations from previous works. The comparisons show that the new 1D-NCL equations have a better agreement with test results, especially at high plasticity soils. Two montmorillonite soils (calcium and sodium types) reported in [36] were used for the verification. The results show that the predicted NCL's using the proposed equations in this study fit connotatively and qualitatively well with the experimental data.

Funding information: Authors state no funding involved.

Author contributions: All authors have accepted responsibility for the entire content of this manuscript and approved its submission.

Conflict of interest: Authors state no conflict of interest.

References

[1] Al-Badran Y, Schanz T. Soil-water characteristic curve and consolidation for fine-grained soils. 4th Asia-Pacific Conference on Unsaturated Soils; 2009 Nov 23–25; Newcastle, Australia. Australian Geomechanics Society; 2009a. p. 243–9.
[2] Al-Badran Y. Volumetric yielding behavior of unsaturated fine-grained soils [dissertation]. Bochum: Ruhr Universität Bochum; 2011.
[3] Ho DYF, Fredlund DG, Raharadjo H. Volume change indices during loading and unloading of an unsaturated soil. Can Geotec J. 1992;29:195–207.
[4] Fredlund DG, Rahardjo H. Soil mechanics for unsaturated soils. New York: John Wiley & Sons; 1993.
[5] Marcial D, Delage P, Cui YJ. On the high stress compression of bentonites. Can Geotech J. 2002;39:812–20.
[6] Baille W, Tripathy S, Schanz T. Swelling pressure and one-dimensional compressibility behaviour of bentonite at large pressure. Appl Clay Sci. 2010;48(3):324–33.
[7] Tripathy S, Sridharan A, Schanz T. Swelling pressures of compacted bentonites from diffuse double layer theory. Can Geotech J. 2004;41:437–50.
[8] Tripathy S, Schanz T. Compressibility behaviour of clays at very large pressures. Can Geotech J. 2007;44(3):355–62.
[9] Griffiths FJ, Josi RC. Change in the pore size distribution due to consolidation of clays. Géotechnique. 1989;39(1):159–67.
[10] Arifin YF. Thermo-hydro-mechanical behavior of compacted bentonite-sand mixtures: An experimetal study [dissertation]. Weimar: Bauhaus-Universität Weimar; 2008.
[11] Nagaraj TS, Murthy Srinivasa BR. A critical reappraisal of compression index equations. Géotechnique. 1986;36(1):27–32.
[12] Skempton AW. The consolidation of clays by gravitational compaction. Q J Geol Sot. 1970;125:373–411.
[13] Skempton AW. Notes on compressibility of clays. Qtrly J Geol Soc Lond. 1944;100(2):119–35.
[14] Terzaghi K, Peck RB. Soil mechanics in engineering practice. New York: John Wiley & Sons. Inc; 1948.
[15] Nishida Y. A brief note on compression index of soils. J SMFE Div ASCE July. 1956;82(2):1–14.
[16] Hough BK. Basic soil engineering. New York: Ronald; 1957.
[17] Azzouz AS, Krizek RJ, Corotis RB. Regression analysis of soil compressibility. Soils Found. 1976;16(2):19–29.
[18] Bowles JW. Physical and geotechnical properties of soils. New York: McGraw Hill; 1979.
[19] Rendon-Herrero O. Universal compression index equation. J Geotech Eng Div. 1980;106:1179–99.
[20] Mayne PW. Cam-Clay Predictions of Undrained Strength. J Geotech Eng Division. Nov 1980;106(GT11).
[21] Koppula SD. Statistical estimation of compression index. ASTM Georech Test J. 1981;4(2):68–73.
[22] Burland JB. On the compressibility and shear strength of natural clays. Géotechnique. 1990;40(3):329–78.
[23] Nath A, DeDalal SS. The role of plasticity index in predicting compression behaviour of clays. EJGE. 2004;9:1–7.
[24] Al-Khafaji A. Empirical compression index equations. International workshop on Innovations in materials and design in civil infrastructure; 2005 Dec 28–29; Cairo, Egypt. p. 1–4.
[25] Herrero OR. Universal compression index equation. J Geotech Eng Division, ASCE. Nov 1980;106(GT11).
[26] Herrero OR. Universal compression index equation; Closure. J Geotech Eng Division. Nov 1983;106(GT11).
[27] Atomic Energy of Canada Limited (AECL). Waste disposal concept; 2002. www.aecltechnologies.com.
[28] Enviros. The virtual repository of nuclear information. Enviros Consulting Ltd., UK; 2003. www.enviros.com/vrepository.
[29] Al-Mukhtar M, Qi Y, Alcover J-F, Bergaya F. Oedometric and water-retention behavior of highly compacted unsaturated smectites. Can Geotech J. 1999;36:675–84.
[30] Fleureau JM, Verbrugge JC, Huergo PJ, Correia AG, Kheirbek-Saoud S. Aspects of the behaviour of compacted clayey soils on drying and wetting paths. Can Geotech J. 2002;39:1341–57.
[31] Al-Badran Y, Schanz T. Yielding surface model of volume change for fine-grained soils. 4th Asia-Pacific Conference on Unsaturated Soils; 2009 Nov 23-25; Newcastle, Australia. Australian Geomechanics Society; 2009b. p. 863–71.
[32] Lambe TW, Whitman RV. Soil mechanics. 3.4. New York: Wiley; 1979. p. 33.
[33] Fredlund DG, Pham QH. Independent Roles of the Stress State Variables on Volume–Mass Constitutive Relations. In: Schanz T, editor. Theoretical and Numerical Unsaturated Soil Mechanics. Berlin, Heidelberg: Springer; 2007.
[34] Vanapalli SK, Fredlund DG, Pufahl DE. The influence of soil structure and stress history on the soil-water characteristic of a compacted till. Géotechnique. 1999;49(2):143–59.
[35] Leong EC, Wee HS, Rahardjo H. One-dimensional compressibility of unsaturated soils. Proceedings of 3rd Asian Conference of Unsaturated Soils; 2007 Apr 21–23; Nanjina, China. p. 237–42.
[36] Mesri G, Olson RE. Consolidation characteristics of montmorillonite. Géotechnique. 1971;21(4):341–52.